Geophysical Research Letters

RESEARCH LETTER
10.1029/2025GL119033

Fluid Stretching at Facies Interfaces Governs Solute Transport

Mohamad Reza Soltanian[1,2], Corey D. Wallace[3], Felipe P. J. de Barros[4], Zhenxue Dai[5], and Kenneth C. Carroll[6]

[1]Department of Geosciences, University of Cincinnati, Cincinnati, OH, USA, [2]Department of Environmental Engineering, University of Cincinnati, Cincinnati, OH, USA, [3]RSI EnTech, Grand Junction, CO, USA, [4]Sonny Astani Department of Civil and Environmental Engineering, University of Southern California, Los Angeles, CA, USA, [5]College of Construction Engineering, Jilin University, Changchun, China, [6]Plant and Environmental Sciences Department, New Mexico State University, Las Cruces, NM, USA

Key Points:

- Facies interfaces act as persistent mixing fronts
- Kinematic deformation metrics explain why cross-facies transitions control plume structure, mixing, and dilution
- Sedimentary architecture governs dispersion and dilution, underscoring the need to resolve interfaces for prediction and remediation

Supporting Information:

Supporting Information may be found in the online version of this article.

Correspondence to:

M. R. Soltanian,
soltanma@uc.edu

Citation:

Soltanian, M. R., Wallace, C. D., de Barros, F. P. J., Dai, Z., & Carroll, K. C. (2025). Fluid stretching at facies interfaces governs solute transport. *Geophysical Research Letters*, *52*, e2025GL119033. https://doi.org/10.1029/2025GL119033

Received 13 SEP 2025
Accepted 15 NOV 2025

Author Contributions:

Conceptualization: Mohamad Reza Soltanian
Data curation: Mohamad Reza Soltanian
Formal analysis: Corey D. Wallace
Funding acquisition: Mohamad Reza Soltanian
Investigation: Mohamad Reza Soltanian
Methodology: Mohamad Reza Soltanian, Corey D. Wallace, Felipe P. J. de Barros, Zhenxue Dai, Kenneth C. Carroll
Project administration: Mohamad Reza Soltanian
Resources: Mohamad Reza Soltanian
Software: Mohamad Reza Soltanian, Corey D. Wallace
Supervision: Mohamad Reza Soltanian
Validation: Mohamad Reza Soltanian, Corey D. Wallace
Visualization: Mohamad Reza Soltanian, Corey D. Wallace

Abstract This study provides a kinematic explanation for why facies interfaces dominate solute transport in heterogeneous aquifers. Using flow and transport simulations, we apply kinematic metrics to quantify deformation processes that control plume evolution. Results show that strong conductivity contrasts generate preferential flow corridors, while transitional zones at facies interfaces act as persistent mixing fronts where stretching and folding intensify mixing. These cross-facies transitions emerge as the primary controls on transport observables such as dispersion and dilution, with within-facies variability exerting secondary effects. By linking sedimentary architecture to flow deformation, this work provides the mechanistic justification for earlier findings that cross-transition probabilities govern solute spreading. The results highlight the need to resolve geologic interfaces in both field characterization and remediation design. Flow topology offers a unifying framework for predicting transport in aquifers and points to opportunities for geophysical methods to target the key architectural features that regulate mixing and dilution.

Plain Language Summary Groundwater contamination is difficult to predict because aquifers are made of different types of sediments with contrasting properties. In this study we use computer models to show that the boundaries (interfaces) between sediments such as coarse sands and fine sands or silts are the main zones where mixing occurs. These interfaces create stretching and folding in the flow field, which intensifies dilution and controls how contaminant plumes spread. Smaller variations within a single sediment type have only minor effects compared to these larger-scale boundaries. By explaining why sediment interfaces dominate transport, this work highlights which geologic features are most important to characterize. The results can help improve groundwater monitoring, remediation design, and the use of geophysical tools to detect the subsurface structures that regulate mixing and dilution.

1. Introduction

Shallow glacial and fluvial aquifers are vital freshwater resources, particularly where surface water sources are scarce or highly variable. These aquifers often contain permeable sedimentary deposits that make them highly responsive to hydrologic changes but also susceptible to anthropogenic impacts (Wallace & Soltanian, 2021a, 2021b). The dynamics of solute transport in such systems are strongly influenced by the spatial arrangement of sedimentary facies types and the associated heterogeneity in hydraulic conductivity, K, which together control the direction and magnitude of the subsurface flow field and regulate processes such as dispersion, dilution, and mixing (de Barros et al., 2015; Soltanian et al., 2020). In heterogeneous porous media, mixing arises not only from plume spreading but from complex interactions among advection, diffusion, and dispersion, which are central to the fate of contaminants (Dentz & Hyman, 2023). Understanding these coupled processes is therefore imperative for effective groundwater management and contamination mitigation, as the physical structure of the aquifer can fundamentally alter the transport of water and solutes, and thus must be mechanistically linked to aquifer architecture (Carroll et al., 2024).

As shown in de Barros et al. (2012), kinematic features of the subsurface flow, defined by the interactions among strain (stretching), shear, and rotation (vorticity), provide a mechanistic measure of mixing potential in heterogeneous aquifers. Since its application to groundwater systems (de Barros et al., 2012), the Okubo–Weiss parameter (Okubo, 1970), denoted here by OW, has been increasingly used to characterize flow in the

Writing – original draft: Mohamad Reza Soltanian, Corey D. Wallace, Felipe P. J. de Barros, Zhenxue Dai, Kenneth C. Carroll
Writing – review & editing: Mohamad Reza Soltanian, Corey D. Wallace, Felipe P. J. de Barros, Zhenxue Dai, Kenneth C. Carroll

subsurface environment. Positive values of OW denote strain-dominated regions and negative values denote rotation-dominated regions. Regions of high OW enhance solute mixing through fluid strain, while rotation-dominated regions suppress mixing and confine plume migration through folding (de Barros et al., 2012). Recently, Basilio Hazas et al. (2022) has provided experimental evidence on the validity of the theoretical work derived in de Barros et al. (2012) linking flow topology to mixing. Sedimentary architecture governs the spatial organization of the K-field which in turn produces the variable strain and rotation patterns that reflect on flow-topology maps. Because plumes encounter a sequence of deformation events as they migrate, the cumulative effect of these events dictates their overall mixing state (de Barros et al., 2012; Dentz et al., 2018; Le Borgne et al., 2013). To represent this cumulative effect, de Barros et al. (2012) introduced an effective OW that integrates weighted deformation events over time. Contrasts in K created by facies boundaries also generate lamellar structures, where fluid elements are repeatedly stretched and folded, enhancing diffusive mass transfer and scalar mixing (Le Borgne et al., 2015; Rolle & Le Borgne, 2019). These processes highlight how sedimentary architecture, through its control of the K field, fundamentally shapes solute dispersion and dilution in shallow aquifers vulnerable to surface-derived contamination.

Depositional processes create interfaces between unconsolidated sediments that produce strong heterogeneity and intricate lithologic stratigraphy. These boundaries not only shape flow dynamics but also regulate biogeochemical processes such as the transport and transformation of organic carbon. As Aeppli et al. (2022) emphasize, interfaces can form localized zones of heightened reactivity where organic carbon is preferentially stored through retention or sorption, or mobilized through dissolution or desorption, with important consequences for groundwater quality. In highly heterogeneous systems, the migration of organic carbon depends on the sediments' physical and geochemical properties, including K, sorptive capacity, microbial composition, and their ability to either promote or suppress solute mixing (Brusseau et al., 2011; DiFilippo et al., 2010; Mohamed et al., 2024). Because these interfaces coincide with sharp K contrasts, they also produce shifts in flow topology, acting as preferential mixing zones where advective and diffusive processes interact to regulate solute spreading (Dentz & Hyman, 2023; Wallace et al., 2021). A representative outcrop showing a distinct interface between low- and high-K units is provided in Figure S1b of Supporting Information S1. Flow deformation and mixing at these facies boundaries can enhance redox turnover and organic-carbon transformations, creating biogeochemical hot spots where reactive solutes and microbial activity are concentrated (Wallace et al., 2021). This coupling between flow deformation and biogeochemical reactivity provides a direct link between flow topology and contaminant attenuation in heterogeneous aquifers. The coupled influence of flow deformation and biogeochemical reactivity at facies boundaries therefore exerts first-order control on contaminant fate, with direct implications for natural attenuation, engineered remediation, and groundwater resource management under anthropogenic stress.

In this study, we provide a kinematic explanation for why sedimentary interfaces dominate solute transport in aquifers. Building on earlier work linking cross-facies transitions to dilution and dispersion (Ren et al., 2022; Ritzi Jr & Soltanian, 2015; Soltanian et al., 2020) and using the concepts introduced in de Barros et al. (2012), we use high resolution numerical simulations with varying levels of heterogeneity to quantify how sedimentary architecture controls topological structure of the flow field and consequently mixing of the solute plume with the ambient fluid. Flow deformation is characterized using both Eulerian and Lagrangian metrics, including the OW parameter, strain rate tensor (SRT), Lagrangian measure of fluid stretching (SL), and finite time Lyapunov exponent (FTLE). These measures will help in revealing how facies boundaries shape plume structure and transport observables such as dispersion and dilution through processes of stretching, stirring, and folding (Dentz & Hyman, 2023). While earlier works identified cross-transition probabilities (i.e., probability of transitioning from one facies to another) as statistical predictors of dispersion and dilution (Ramanathan et al., 2010; Soltanian et al., 2020; Soltanian, Ritzi, Dai, et al., 2015), here we provide a kinematic justification by showing that facies interfaces are the persistent *loci* of stretching, shear, and rotation. This establishes a mechanistic link between geologic structure and transport observables, explaining why cross-facies transitions consistently dominate plume behavior across heterogeneous aquifers. By integrating these flow topology metrics with detailed facies-based heterogeneity models, this work advances understanding of the role of geologic interfaces as persistent mixing fronts, providing mechanistic insight that informs both predictive modeling and the design of more effective remediation strategies in contaminated aquifers.

2. Methods

2.1. Representation of Sediment Heterogeneity

Sediments in shallow unconfined alluvial aquifers often exhibit complex, multiscale stratification, with nested facies composed of smaller-scale assemblages (Dai et al., 2004). This hierarchical structure reflects the depositional environment of the aquifer, which gives rise to diverse lithologic sequences and varying degrees of heterogeneity. The resulting facies architecture governs spatial variability in key sediment attributes, such as K and porosity, and ultimately controls groundwater flow patterns and solute transport dynamics. In this study, sediment heterogeneity is represented using a series of two-dimensional (2D) models consisting of two facies types: higher-K and lower-K. The Cartesian coordinate system is $\mathbf{x} = (x_1, x_2)$. A conceptual illustration of the heterogeneity representations used is shown in Figure S1 of Supporting Information S1. The hierarchical facies structure is generated using the transition probability–based approach in T-PROGS (Carle, 1999). The models are composed of medium sand representing higher-K facies and fine sand and silt representing lower-K facies. Approximately 9,800 indicator data points, including volume proportions (0.39 for high-K and 0.61 for low-K facies) and mean facies lengths (3.0 m for high-K and 5.85 m for low-K facies), were used to produce conditional realizations. These data, derived from detailed field characterization at the Borden site and consistent with prior studies (Soltanian et al., 2020; Soltanian, Ritzi, Huang & Dai, 2015a, 2015b), were used to develop Markov-chain transition-probability models in both vertical and horizontal directions.

To systematically investigate the relative contributions of meter-scale architecture (i.e., the geometry and arrangement of contrasting facies) and in-facies variability on solute spreading and dilution, we designed four conceptual cases that incrementally introduce complexity in the heterogeneity structure:

- *Case B*: *Binary Heterogeneity with Uniform K*—This case represents a simple binary field with uniform higher-K and lower-K facies. The higher-K facies is assigned a permeability of 4.74×10^{-11} m^2, while the lower-K facies has a permeability of 2.11×10^{-11} m^2. Each facies is internally homogeneous, meaning there is no variability in K within the high- or low-K zones. While individual facies are uniform, the overall domain is heterogeneous due to the contrast between the higher- and lower-K facies. This case serves as a baseline scenario, where heterogeneity is solely controlled by the meter-scale arrangement and boundaries of the two facies types.
- *Case B-infacies*: *Binary Heterogeneity with In-Facies Heterogeneity*—In this case, the higher-K and lower-K zones in the binary heterogeneity distribution exhibit in-facies K heterogeneity. The K within each facies follows a log-normal distribution, with a variance of 0.25 for the higher-K facies and 0.17 for the lower-K facies. This case introduces realistic small-scale variability within each facies, allowing us to evaluate the role of internal heterogeneity independent of enhanced contrast across the facies.
- *Case En-B: Enhanced Binary Heterogeneity*—Here the binary heterogeneity distribution from Case B is maintained, but the higher-K facies is assumed to be more conductive than the lower-K facies. Specifically, the K of the higher-K facies is increased by a factor of 10 compared to the lower-K facies, which enhances the contrast in K between the two facies types. This scenario isolates the effect of enhanced K contrast on flow channelization and solute spreading, while keeping within-facies properties uniform.
- *Case En-B-infacies: In-Facies Heterogeneity with Enhanced Higher-K Conductivity*—This case combines the features of Case B-infacies and Case En-B, where both the higher-K and lower-K facies exhibit in-facies heterogeneity, as in Case B-infacies, and the higher-K facies has its conductivity increased by a factor of 10, as in Case En-B. This provides a highly heterogeneous K field, both within the facies and the contrast between higher-K and lower-K regions. This configuration enables the assessment of how internal small-scale heterogeneity interacts with strongly contrasting facies geometries to influence transport dynamics.

These four cases are designed to isolate the relative effects of facies architecture, K contrast, and in-facies variability on groundwater flow and solute transport. Flow and transport simulations were performed using PFLOTRAN (Lichtner et al., 2015), and complete numerical details of the model configuration are provided in the Text S1 of Supporting Information S1.

2.2. Fluid Deformation Metrics

In this section, we present several key fluid deformation-based metrics used to analyze the topology of the flow field in heterogeneous aquifers and quantify its connection with transport observables. Variations in sediment

properties (e.g., K) both within and across facies, generate spatially variable pore water velocity fields. These velocity fields are complex and create significant spatial and temporal variability that enrich the transport dynamics in groundwater systems. Traditional flow nets composed of streamlines and equipotential lines provide only a static representation of the velocity field and therefore do not capture the deformation dynamics that govern how solutes are stretched, folded, and dispersed through time (Ottino, 1989). To characterize these dynamic processes, we apply several metrics that are based on fluid deformation rates, including the OW, SRT, SL, and FTLE. Together, these metrics quantify fundamental deformation mechanisms such as rotation, shear, and stretching, which directly control mixing and the evolution of solute plumes in groundwater as shown in de Barros et al. (2012). By resolving the structure of the velocity field and identifying regions of enhanced deformation, these measures provide a more detailed and predictive framework for understanding transport behavior in complex flow environments.

We apply multiple, complementary metrics to capture distinct aspects of flow deformation. The OW parameter provides an Eulerian, instantaneous view of strain, shear, and vorticity; the SRT quantifies local deformation directly; SL integrates deformation history along fluid trajectories; and the FTLE highlights particle separation over finite time intervals. Using these together ensures that our interpretation of mixing processes is not biased by the limitations of any single metric, but rather reflects consistent patterns across local and cumulative perspectives.

Okubo-Weiss Parameter: The OW parameter (Okubo, 1970; Weiss, 1991) characterizes the geometrical properties of fluid streamlines by considering both normal (linear deformation, such as stretching or compression) and shear (angular deformation) strains, along with vorticity. The OW metric is related to the determinant of the velocity gradient tensor. The OW metric is expressed as:

$$\mathrm{OW} = -4\det(\boldsymbol{\epsilon}), \tag{1}$$

where the velocity gradient tensor $\boldsymbol{\epsilon}$ is given by $\epsilon_{ij} \equiv \partial v_i/\partial x_j$.

In hydrological applications, de Barros et al. (2012) used the OW metric to relate subsurface flow kinematics to solute mixing. Their work showed how global mixing rates, measured through the dilution index (Kitanidis, 1994), are influenced by the history of flow deformation events captured in the OW parameter. Following the work of (Geng et al., 2020), we use the standard deviation of the OW field (denoted σ_{OW}) to classify subsurface flow regions into strain-dominated ($\mathrm{OW} > 0.2\sigma_{\mathrm{OW}}$) and vorticity-dominated ($\mathrm{OW} < -0.2\sigma_{\mathrm{OW}}$) areas. A transitional region characterized by small positive and negative values of OW ($|\mathrm{OW}| \leq 0.2\sigma_{\mathrm{OW}}$) represents shear strain dominance. We quantify the areal extent of these strain- and vorticity-dominated fields and evaluate the relative contributions of each facies type. Having a map of the OW values is important because, as shown by (de Barros et al., 2012), the dilution rates of a solute plume will depend on whether the straining, shearing or vorticity dominates. Experimental works showed how the OW metric can be used as a predictor for mixing (Basilio Hazas et al., 2022; Ziliotto et al., 2025).

Strain Rate Tensor: The SRT measures the rate at which a fluid element is stretched or compressed, helping to characterize fluid deformation and predict the evolution of fluid flows. The SRT is defined as (Kundu et al., 2024):

$$\mathrm{SRT} = \frac{1}{2}\left(\boldsymbol{\epsilon} + (\boldsymbol{\epsilon})^T\right) \tag{2}$$

Lagrangian Stretching: To predict transport hotspots without simulating transport directly, we use SL, which characterizes the cumulative deformation experienced by a fluid element along its trajectory. The deformation gradient $\mathbf{F}(T)$ maps an infinitesimal separation vector from its initial to its advected state after a finite travel time T, and the associated right Cauchy–Green tensor is $\mathbf{C}(T) = \mathbf{F}^{\top}\mathbf{F}$. The Lagrangian stretching factor is then:

$$\mathrm{SL}(T) = \sqrt{\lambda_{\max}(\mathbf{C}(T))}, \tag{3}$$

where $\lambda_{\max}$ is the largest eigenvalue of $\mathbf{C}$. SL thus represents the maximum elongation of a fluid element over the observation horizon. Unlike purely Eulerian diagnostics such as the strain-rate tensor or the OW parameter, SL

accumulates the entire deformation history of a trajectory, highlighting persistent mixing fronts and transport pathways that cannot be inferred from instantaneous measures alone.

Finite-Time Lyapunov Exponent: The FTLE quantifies the average exponential stretching of fluid elements over a finite time interval, providing a measure of how rapidly initially close particle trajectories diverge. Following Yoon et al. (2021), we compute the FTLE directly from the Cauchy–Green deformation tensor, using the same framework as the SL. The FTLE is obtained by normalizing the logarithm of the stretching factor by the integration time:

$$\sigma(T) = \frac{1}{T} \ln(\mathrm{SL}(T)). \tag{4}$$

Our flow fields are steady-state but computed at discrete output intervals $\Delta t = 2$ days. To evaluate $\mathbf{F}(T)$ incrementally from velocity gradients, we use the first-order approximation:

$$\mathbf{F} \approx \mathbf{I} + \Delta t\, \boldsymbol{\epsilon}, \tag{5}$$

where $\mathbf{I}$ is the identity tensor and $\epsilon_{ij} = \partial v_i / \partial x_j$ is the local velocity gradient tensor derived from PFLOTRAN velocity outputs. This approximation is standard when grid-scale velocity fields are available (Engdahl et al., 2014). We accumulate the effect of deformation over successive time steps to construct $\mathbf{C}(T)$ and then evaluate $\lambda_{\max}$.

While SL measures the maximum elongation of a fluid element after a finite time T, FTLE converts that elongation into a rate. This distinction allows FTLE to highlight spatial regions of high mixing intensity and persistent particle separation, complementing Eulerian measures such as the SRT or the OW parameter.

2.3. Global Transport Metrics

To evaluate how sedimentary architecture influences solute spreading and dilution at the domain scale, we analyze three transport descriptors: the trajectory of the plume's center of mass, displacement variance (which is directly linked to dispersion), and the natural logarithm of the dilution index, $\ln[E(t)]$. The trajectory of the plume's center of mass, which corresponds to the first central moment of the solute body, is a localized metric that describes the average position of the plume and highlights the influence of higher conductivity pathways on plume velocity. The displacement variance, representing the second central moment, captures plume spreading and reveals how structural contrasts in hydraulic conductivity lead to enhanced dispersion across the domain. The third metric, $\ln[E(t)]$, is the natural logarithm of the dilution index $E(t)$, which quantifies the effective volume occupied by the solute plume. This entropy-based measure accounts for both solute spreading and local scale mixing and has been widely adopted as a proxy for dilution efficiency in heterogeneous systems (Kitanidis, 1994). The natural logarithm is applied to improve interpretability and to express the exponential growth behavior typically observed in scalar mixing under heterogeneous flow conditions. As shown in de Barros et al. (2012), in heterogeneous fields, regions dominated by strain and shear accelerate the growth of $\ln[E(t)]$, indicating enhanced scalar mixing, while regions dominated by rotation hinder dilution. Thus, $\ln[E(t)]$ links local flow structure to global mixing behavior and enables a robust assessment of how sedimentary structure governs solute spreading and dilution across the aquifer. The mathematical formulations of these global metrics, the plume's center of mass, the second central moment, and E(t) are provided in the Text S2 of Supporting Information S1.

3. Results and Discussion

The spatial variability in mixing metrics (Figure 1) illustrates how different representations of sediment heterogeneity alter the underlying flow structure and influence solute transport behavior. In the binary facies model (B) and the binary model with within-facies variability (B-infacies), the K fields exhibit limited contrast between the high- and low-K facies (Figure 1a). This results in relatively small velocity gradients and broad, low-intensity regions of flow deformation, as indicated by smoother strain rate and stretching metrics (Figures 1c and 1d). In comparison, when the K contrast is increased in the enhanced binary model (En-B), where the high-K facies is increased tenfold relative to the low-K facies, more distinct high-conductivity corridors form. These corridors promote faster fluid movement and produce concentrated zones of strain and stretching along preferential flow

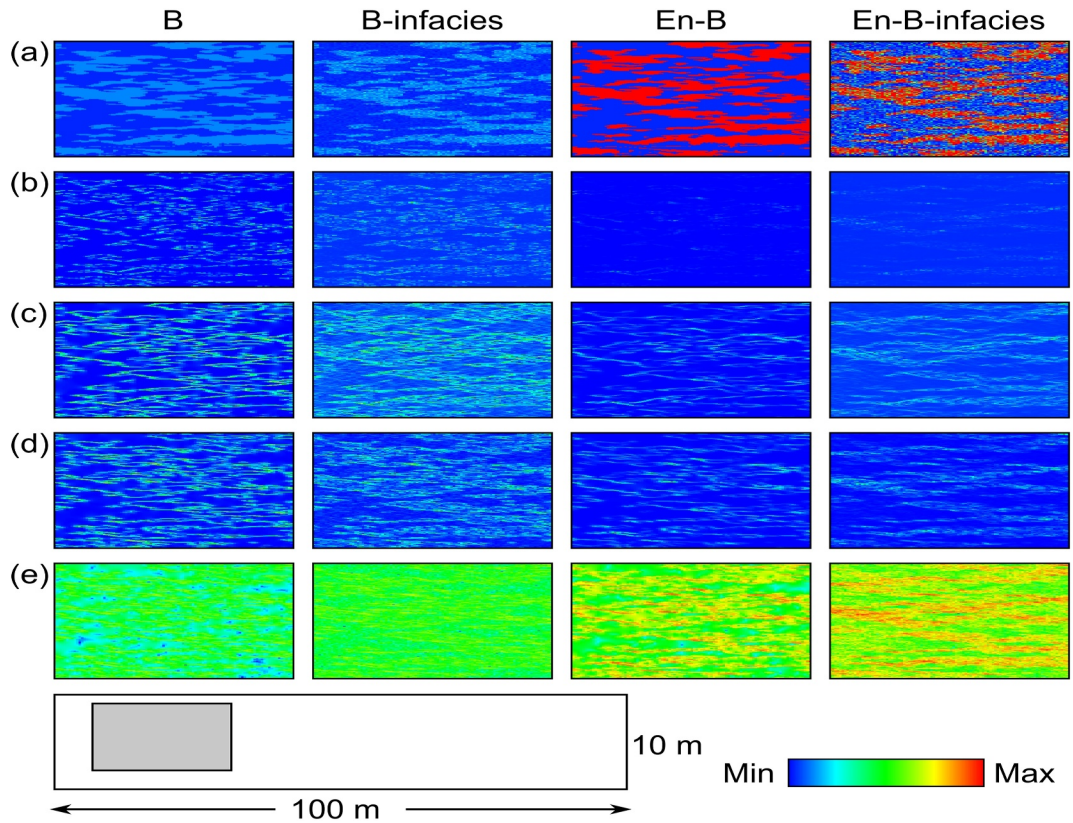

Figure 1. Spatial distribution of key flow topology and deformation metrics. (a) Natural logarithm of hydraulic conductivity, (b) Okubo-Weiss (OW) parameter highlighting zones of strain and vorticity, (c) strain rate tensor (SRT) indicating regions of fluid deformation, (d) Lagrangian stretching rate (SL) reflecting cumulative fluid element elongation, (e) finite-time Lyapunov exponent (FTLE) showing regions of high fluid particle separation. For each metric, the color bar represents a normalized scale where the maximum value within the data set is set to 1 and all other values are scaled proportionally between 0 and 1. Normalization is performed per metric and per case to emphasize spatial patterns; absolute magnitudes differ across metrics. The color maps are consistent across all cases to facilitate visual comparison of flow topology and mixing characteristics driven by sediment heterogeneity. All metrics were computed across the full 100 m × 10 m model domain, but the visualizations are shown for a smaller subsection (approximately 25 m × 8 m) to better illustrate facies interfaces and the corresponding flow topology and deformation patterns.

paths (Figures 1c and 1d). The most pronounced flow deformation is observed in the En-B-infacies model, where both large-scale facies contrasts and small-scale internal variability generate highly heterogeneous velocity fields with sharp local gradients. This leads to localized regions of intense stretching, expressed by elevated values of SRT (Figure 1c), SL (Figure 1d), and most extensively in the FTLE field (Figure 1e). Collectively, the spatial organization of these metrics shows that both the contrast between facies and the heterogeneity within facies influence the magnitude and distribution of flow deformation, which in turn affects the solute mixing potential throughout the domain.

The influence of sediment structure on flow deformation is further revealed by examining Eulerian measures of fluid stretching (Figure 1d). In the more homogeneous cases (B and B-infacies), fluid parcels experience moderate stretching, which limits the potential for dispersion. In contrast, simulations with enhanced contrast (En-B and En-B-infacies) exhibit intensified and spatially coherent stretching aligned with higher conductivity channels, promoting rapid plume elongation and increased dispersive spreading. The En-B-infacies scenario shows elevated stretching rates that persist throughout the simulation, illustrating how fine-scale heterogeneity can amplify deformation initiated by broader facies contrasts. These elevated stretching rates contribute to the formation of elongated zones where solute concentrations experience continuous stretching and folding, thereby increasing the interfacial area between different solute concentrations and enhancing mixing through diffusion. To support the role of interfaces in controlling flow topology, we quantify the length and density of boundaries

between contrasting facies throughout the domain. The results show that scenarios with greater interface density correspond to more pronounced stretching patterns and deformation zones, confirming that the spatial arrangement and abundance of facies interfaces strongly influence flow structure and solute mixing behavior. The consistency of results across OW, SRT, SL, and FTLE reinforces that interfaces and high-contrast corridors are systematically captured as deformation hotspots. Although each metric emphasizes different aspects, the spatial patterns agree. This consistency demonstrates that our conclusions are robust and not artifacts of a single diagnostic tool. The convergence of results confirms that interfaces and high-contrast corridors are systematically captured as deformation hotspots, highlighting their role as persistent mixing fronts.

The temporal evolution of the key transport quantities provides a deeper insight into the relationship between K heterogeneity and plume spreading and mixing (Figure S2 in Supporting Information S1). Throughout the simulation period, plume metrics such as center-of-mass position and second central moment indicate that models with strong K contrasts promote faster plume migration and broader spreading (see Figure S2 in Supporting Information S1, top and middle panels). Both the En-B and En-B-infacies cases display early and sustained plume advancement, whereas the B-infacies case progresses more gradually but still shows increased spreading as a result of the influence of small-scale variability. In contrast, within facies heterogeneity exerts only a modest influence on transport speed and mixing compared to the cases with strong contrasts, highlighting the dominant role of facies architecture and the structure of transitions between facies. These patterns confirm that both global and local heterogeneity govern not only the rate of plume migration but also its internal structure, which becomes progressively stretched, folded, and dispersed in the simulations with more complex heterogeneity. The $\ln(E(t))$ metric (Figure S2 in Supporting Information S1, see bottom panel) reinforces this conclusion by demonstrating that dilution is primarily controlled by large-scale sedimentary architecture rather than small-scale variability alone. For example, the B and B-interface cases, which lack strong contrasts in hydraulic conductivity, yield nearly identical values of $\ln(E(t))$, indicating limited enhancement of dilution. In contrast, both En-B and En-B-infacies models show elevated $\ln(E(t))$ over time, reflecting more efficient mixing facilitated by pronounced K contrasts and well-connected preferential pathways. These results are consistent with the findings of Soltanian et al. (2020) and Ren et al. (2022), who demonstrated that scalar mixing and solute dilution are controlled primarily by meter-scale sedimentary structure. While intra-facies heterogeneity introduces additional small-scale velocity variability, its influence on global metrics such as the dilution index or plume variance (i.e., second central spatial moment) remains secondary.

To further quantify the balance between strain, shear and rotation across the domain, we focus on the OW parameter. The OW metric provides a natural classification of flow regions into strain-, shear-, and rotation-dominated regimes. For each case, we calculate the total area of grid cells assigned to each OW regime and report this as the cumulative area of strain-, shear-, and vorticity-dominated zones (Figure 2). Vorticity is comparatively small relative to strain and shear across cases, confirming that strain and shear dominate flow deformation. In higher K regions (Figure 2a), the cumulative area of strain-dominated cells is large for every case, with the B-infacies model showing the highest value, followed by En-B-infacies, B, and En-B. Shear-dominated areas, by contrast, are greatest for En-B, followed by B, En-B-infacies, and B-infacies. This indicates that both internal variability and enhanced contrasts amplify stretching, but in different ways: B-infacies increases the extent of strain-dominated regions, while En-B intensifies shear along K corridors. In lower K regions (Figure 2b), strain-dominated areas remain substantial, though the ranking shifts: En-B-infacies is slightly higher than B-infacies, followed by B, while En-B is notably lower. Shear-dominated areas are largest for En-B, followed by B, with B-infacies and En-B-infacies nearly equal but smaller. These results suggest that even low-K zones experience significant deformation when facies contrasts are strong or when internal variability is present. Facies interfaces (Figure 2c) show much smaller cumulative areas overall compared to other zones, but they consistently exhibit both strain and shear, with B producing the highest strain and En-B-infacies the highest shear. This reinforces that although interfaces occupy a relatively small portion of the domain, they serve as critical mixing fronts. Within facies interiors (Figure 2d), the rankings again diverge: strain is highest for B-infacies, then B, En-B-infacies, and En-B, while shear is dominated by En-B, followed by En-B-infacies, B, and B-infacies. These patterns demonstrate that intra-facies variability intensifies strain, whereas enhanced K contrast primarily strengthens shear. Together, the cumulative area analysis shows how architecture and internal variability act through different deformation modes, and why facies interfaces, despite their small footprint, exert strong control on plume mixing and dilution. Interfaces are thus the loci where strain and shear coexist, making them persistent

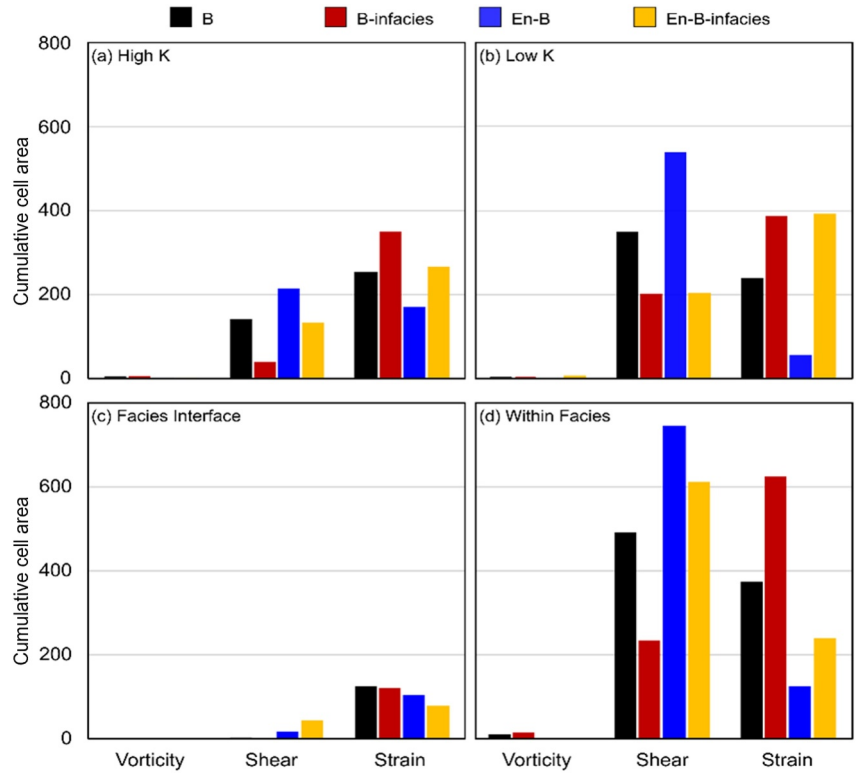

Figure 2. Bar plots showing the cumulative area of cells classified into the three OW regimes: strain-dominated, vorticity-dominated, and shear zones. For each case, the cumulative area denotes the total grid cell area belonging to each OW regime. Areas are computed separately for (a) higher-K regions, (b) lower-K regions, (c) facies interfaces, and (d) within-facies zones. The results highlight how enhanced contrast and internal heterogeneity influence the spatial extent of flow deformation and mixing potential across different sedimentary domains.

mixing fronts. This provides the kinematic justification for earlier findings that cross-transition probabilities dominate solute transport (Soltanian, Ritzi, Huang & Dai, 2015a, 2015b).

These observations align with earlier theoretical work showing that sedimentary architecture and cross-transition probabilities (i.e., probability of transitioning from one facies to another) largely define the shape and range of spatial correlation structures (Ritzi Jr & Allen-King, 2007). Building on this foundation, Soltanian et al. (2015a); Soltanian et al. (2015b) developed Lagrangian-based transport models that decompose displacement variance (i.e., second central moment), dispersivity, retardation factor, and dilution index into contributions from auto- and cross-transition probabilities. These studies revealed that cross-facies transitions at larger scale architecture are primary controls on solute spreading and mixing. Soltanian et al. (2020) extended this framework with a semi-analytical solution for the dilution index, showing how cross-facies transitions at multiple scales regulate the temporal scaling of dilution. Complementing these Lagrangian approaches, Ren et al. (2022) used detailed numerical simulations of multiscale facies architectures to confirm that sedimentary structure strongly governs effective dispersion, while mixing is comparatively less sensitive to fine-scale organization. The present work provides the kinematic justification for these findings, demonstrating why cross-transition probabilities and global transport metrics are controlled by facies architecture, by explicitly linking sedimentary interfaces to persistent zones of strain, shear, and stretching.

Advances in geophysical imaging techniques, particularly those that resolve facies interfaces at scales relevant to aquifer heterogeneity, offer promising opportunities to characterize mixing potential more directly (McGarr et al., 2021). While large-scale seismic methods have long been used in hydrocarbon reservoir characterization and sequence stratigraphy, recent developments in high-resolution and multi-physics approaches now enable improved detection of subsurface heterogeneity in groundwater systems. Field-scale studies have demonstrated that high-resolution electrical resistivity tomography (ERT) and electromagnetic induction (EMI) can delineate conductivity contrasts at facies boundaries and identify zones of enhanced hyporheic mixing and reactivity within

fluvial deposits. These methods, together with shallow seismic imaging, provide a practical means to target the sedimentary interfaces that govern subsurface deformation and mixing. These findings highlight the potential for integrating advanced geophysical techniques with flow and transport models to improve the characterization of sedimentary architecture at contaminated sites. By providing a clearer understanding of how sedimentary features control flow patterns and solute behavior, this approach can help overcome limitations associated with sparse site data. Such improved characterization enables more informed monitoring and remediation decisions, ultimately enhancing predictive capabilities and groundwater management strategies for protecting vital freshwater resources.

Given the hierarchical nature of aquifer heterogeneity and the significant role of bivariate and cross-transition structures, multiscale modeling approaches are essential. Hybrid and multiscale frameworks, such as those described by Scheibe et al. (2015), are valuable because they enable deformation metrics (e.g., Eulerian stretching rates and cumulative OW regime areas) to be represented consistently across scales, ensuring that the effects of facies interfaces and connectivity are not lost during upscaling. By linking observable geophysical features to these physically meaningful parameters, predictive models can be better calibrated, ultimately enhancing targeted remediation strategies and improving the reliability of forward simulations in complex heterogeneous aquifers.

Taken together, the integrated spatial and temporal analyses from flow fields and stretching rates of fluid elements to plume evolution and cumulative OW regime areas offer a comprehensive understanding of how sedimentary architecture governs solute transport in complex aquifers. Representing multiscale heterogeneity is critical for accurately characterizing and predicting transport behavior. This helps explain the longstanding challenges in groundwater remediation efforts, as highlighted by Carroll et al. (2024), who emphasize that improved understanding of multiscale heterogeneity is essential for advancing remediation design and outcomes. In particular, accurate representation must capture both the connectivity of high K corridors, which dictates preferential flow pathways and plume acceleration, and the geometry and distribution of low K zones, which control long-term storage and release through rate-limited mass transfer and backdiffusion. Without resolving these key features, predictions of plume migration patterns, first arrival times, risk, and remediation timescales will be biased, regardless of whether multiscale variability is nominally included. The interaction between conductive corridors, cross-facies interfaces, and internal heterogeneity drives a cascade of deformation processes that control mixing, spreading, and dilution. These deformation processes manifest directly in transport observables such as dispersion and dilution index. Recognizing these multiscale interactions is therefore vital for enhancing model fidelity and for developing more targeted and efficient groundwater management and remediation strategies that address real-world heterogeneity.

Because interfaces, though limited in areal extent, repeatedly coincide with the strongest strain- and shear-dominated zones (Figure 2), they are important yet difficult to capture in sparse site data. Advanced geophysical methods and probabilistic frameworks should therefore prioritize resolving these features. Doing so will directly improve predictions of transport observables such as dispersion and dilution, and guide more effective monitoring and remediation strategies in complex aquifers.

4. Summary

We investigated how sedimentary architecture governs solute transport by quantifying flow deformation in heterogeneous aquifers. This mechanistic perspective allows us to better connect mixing and spreading of solutes with specific kinematical features of the spatially heterogeneous flow. Across geological conceptualizations that varied facies distribution, K contrast, and in-facies variability, the diagnostics consistently showed that architecture exerts primary control on flow, mixing, and dispersion. Strong K contrasts organize high-conductivity corridors that enhance plume spreading rates, while variability within facies adds local deformation that intensifies mixing. Facies interfaces emerge as persistent mixing fronts, concentrating strain and shear and exerting disproportionate control on plume structure, dilution, and effective dispersion. This organization is consistently captured by fluid deformation metrics including the Okubo–Weiss parameter, Eulerian stretching rates, the strain rate tensor, and finite-time Lyapunov exponents, providing a kinematic justification for why facies architecture dictates solute spreading and mixing across scales.

This study provides the mechanistic justification for why cross-transition probabilities, identified in earlier statistical and Lagrangian analyses, govern solute spreading and mixing. By linking geologic structure to flow deformation and transport observables, the results advance understanding of how heterogeneity at multiple scales

regulates contaminant fate and highlight the importance of resolving facies interfaces in site characterization and remediation design.

Inclusion in Global Research Statement

All authors meet AGU authorship criteria. No additional permits or authorizations were required.

Conflict of Interest

The authors declare no conflicts of interest relevant to this study.

Data Availability Statement

The PFLOTRAN input files used in this study are publicly available at Mendeley via Soltanian, R. (2025) (Soltanian, 2025).

Acknowledgments
This research was supported by the National Science Foundation under Grant EAR-2048452. Any opinions, findings, conclusions, or recommendations expressed in this paper are those of the authors and do not necessarily reflect the views of the National Science Foundation. We also acknowledge the intellectual influence of past collaborations with R.W. Ritzi and Y. Rubin, whose insights helped shape the perspectives developed in this study.

References

Aeppli, M., Babey, T., Engel, M., Lacroix, E. M., Tolar, B. B., Fendorf, S., et al. (2022). Export of organic carbon from reduced fine-grained zones governs biogeochemical reactivity in a simulated aquifer. *Environmental Science & Technology*, *56*(4), 2738–2746. https://doi.org/10.1021/acs.est.1c04664

Basilio Hazas, M., Ziliotto, F., Rolle, M., & Chiogna, G. (2022). Linking mixing and flow topology in porous media: An experimental proof. *Physical Review E*, *105*(3), 035105. https://doi.org/10.1103/physreve.105.035105

Brusseau, M., Carroll, K. C., Allen, T., Baker, J., DiGuiseppi, W., Hatton, J., et al. (2011). Impact of in situ chemical oxidation on contaminant mass discharge: Linking source-zone and plume-scale characterizations of remediation performance. *Environmental Science & Technology*, *45*(12), 5352–5358. https://doi.org/10.1021/es200716s

Carle, S. F. (1999). *T-PROGS: Transition Probability Geostatistical Software, version 2.1*. Department of Land, Air and Water Resources, University of California.

Carroll, K. C., Brusseau, M. L., Tick, G. R., & Soltanian, M. R. (2024). Rethinking pump-and-treat remediation as maximizing contaminated groundwater. *Science of the Total Environment*, *918*, 170600. https://doi.org/10.1016/j.scitotenv.2024.170600

Dai, Z., Ritzi, R. W., Jr., Huang, C., Rubin, Y. N., & Dominic, D. F. (2004). Transport in heterogeneous sediments with multimodal conductivity and hierarchical organization across scales. *Journal of Hydrology*, *294*(1–3), 68–86. https://doi.org/10.1016/j.jhydrol.2003.10.024

de Barros, F. P. J., Dentz, M., Koch, J., & Nowak, W. (2012). Flow topology and scalar mixing in spatially heterogeneous flow fields. *Geophysical Research Letters*, *39*(8). https://doi.org/10.1029/2012gl051302

de Barros, F. P. J., Fiori, A., Boso, F., & Bellin, A. (2015). A theoretical framework for modeling dilution enhancement of non-reactive solutes in heterogeneous porous media. *Journal of Contaminant Hydrology*, *175*, 72–83.

Dentz, M., de Barros, F. P. J., Le Borgne, T., & Lester, D. R. (2018). Evolution of solute blobs in heterogeneous porous media. *Journal of Fluid Mechanics*, *853*, 621–646. https://doi.org/10.1017/jfm.2018.588

Dentz, M., & Hyman, J. D. (2023). The hidden structure of hydrodynamic transport in random fracture networks. *Journal of Fluid Mechanics*, *977*, A38. https://doi.org/10.1017/jfm.2023.973

DiFilippo, E. L., Carroll, K. C., & Brusseau, M. L. (2010). Impact of organic-liquid distribution and flow-field heterogeneity on reductions in mass flux. *Journal of Contaminant Hydrology*, *115*(1–4), 14–25. https://doi.org/10.1016/j.jconhyd.2010.03.002

Engdahl, N. B., Benson, D. A., & Bolster, D. (2014). Predicting the enhancement of mixing-driven reactions in nonuniform flows using measures of flow topology. *Physical Review E*, *90*(5), 051001. https://doi.org/10.1103/physreve.90.051001

Geng, X., Boufadel, M. C., Rajaram, H., Cui, F., Lee, K., & An, C. (2020). Numerical study of solute transport in heterogeneous beach aquifers subjected to tides. *Water Resources Research*, *56*(3), e2019WR026430. https://doi.org/10.1029/2019wr026430

Kitanidis, P. K. (1994). The concept of the dilution index. *Water Resources Research*, *30*(7), 2011–2026. https://doi.org/10.1029/94wr00762

Kundu, P. K., Cohen, I. M., Dowling, D. R., & Capecelatro, J. (2024). *Fluid mechanics*. Elsevier.

Le Borgne, T., Dentz, M., & Villermaux, E. (2013). Stretching, coalescence, and mixing in porous media. *Physical Review Letters*, *110*(20), 204501. https://doi.org/10.1103/physrevlett.110.204501

Le Borgne, T., Dentz, M., & Villermaux, E. (2015). The lamellar description of mixing in porous media. *Journal of Fluid Mechanics*, *770*, 458–498. https://doi.org/10.1017/jfm.2015.117

Lichtner, P. C., Hammond, G. E., Lu, C., Karra, S., Bisht, G., Andre, B., et al. (2015). *Pflotran user manual: A massively parallel reactive flow and transport model for describing surface and subsurface processes* (Tech. Rep.). Los Alamos National Laboratory (LANL), Los Alamos, NM (United States).

McGarr, J. T., Wallace, C. D., Ntarlagiannis, D., Sturmer, D. M., & Soltanian, M. R. (2021). Geophysical mapping of hyporheic processes controlled by sedimentary architecture within compound bar deposits. *Hydrological Processes*, *35*(9), e14358. https://doi.org/10.1002/hyp.14358

Mohamed, R. A., Soltanian, M. R., Wang, D., & Carroll, K. C. (2024). Sensitivity of mass flux reduction and mass removal of perfluoroalkyl substances to groundwater flow and transport parameter variability and heterogeneity. *Journal of Hydrology*, *645*, 132268. https://doi.org/10.1016/j.jhydrol.2024.132268

Okubo, A. (1970). Horizontal dispersion of floatable particles in the vicinity of velocity singularities such as convergences. *Deep-Sea Research and Oceanographic Abstracts*, *17*(3), 445–454. https://doi.org/10.1016/0011-7471(70)90059-8

Ottino, J. M. (1989). *The kinematics of mixing: Stretching, chaos, and transport* (Vol. 3). Cambridge University Press.

Ramanathan, R., Ritzi, R. W., Jr., & Allen-King, R. M. (2010). Linking hierarchical Stratal architecture to plume spreading in a Lagrangian-based transport model: 2. Evaluation using new data from the Borden site. *Water Resources Research*, *46*(1). https://doi.org/10.1029/2009wr007810

Ren, W., Ershadnia, R., Wallace, C. D., LaBolle, E. M., Dai, Z., de Barros, F. P., & Soltanian, M. R. (2022). Evaluating the effects of multiscale heterogeneous sediments on solute mixing and effective dispersion. *Water Resources Research*, *58*(9), e2021WR031886. https://doi.org/10.1029/2021wr031886

Ritzi, R. W., Jr., & Allen-King, R. M. (2007). Why did Sudicky [1986] find an exponential-like spatial correlation structure for hydraulic conductivity at the Borden research site? *Water Resources Research*, *43*(1). https://doi.org/10.1029/2006wr004935

Ritzi, R. W., Jr., & Soltanian, M. R. (2015). What have we learned from deterministic geostatistics at highly resolved field sites, as relevant to mass transport processes in sedimentary aquifers? *Journal of Hydrology*, *531*, 31–39. https://doi.org/10.1016/j.jhydrol.2015.07.049

Rolle, M., & Le Borgne, T. (2019). Mixing and reactive fronts in the subsurface. *Reviews in Mineralogy and Geochemistry*, *85*(1), 111–142. https://doi.org/10.2138/rmg.2018.85.5

Scheibe, T. D., Murphy, E. M., Chen, X., Rice, A. K., Carroll, K. C., Palmer, B. J., et al. (2015). An analysis platform for multiscale hydrogeologic modeling with emphasis on hybrid multiscale methods. *Groundwater Series*, *53*(1), 38–56. https://doi.org/10.1111/gwat.12179

Soltanian, M. R. (2025). PFLOTRAN input files for geologically defined interfaces control flow topology and scalar mixing. *Mendeley Data, V1*. https://doi.org/10.17632/tjb9xv4n3j.1

Soltanian, M. R., Behzadi, F., & de Barros, F. P. (2020). Dilution enhancement in hierarchical and multiscale heterogeneous sediments. *Journal of Hydrology*, *587*, 125025. https://doi.org/10.1016/j.jhydrol.2020.125025

Soltanian, M. R., Ritzi, R., Dai, Z., Huang, C., & Dominic, D. (2015). Transport of kinetically sorbing solutes in heterogeneous sediments with multimodal conductivity and hierarchical organization across scales. *Stochastic Environmental Research and Risk Assessment*, *29*(3), 709–726. https://doi.org/10.1007/s00477-014-0922-3

Soltanian, M. R., Ritzi, R. W., Huang, C. C., & Dai, Z. (2015a). Relating reactive solute transport to hierarchical and multiscale sedimentary architecture in a Lagrangian-based transport model: 1. Time-dependent effective retardation factor. *Water Resources Research*, *51*(3), 1586–1600. https://doi.org/10.1002/2014wr016353

Soltanian, M. R., Ritzi, R. W., Huang, C. C., & Dai, Z. (2015b). Relating reactive solute transport to hierarchical and multiscale sedimentary architecture in a Lagrangian-based transport model: 2. Particle displacement variance. *Water Resources Research*, *51*(3), 1601–1618. https://doi.org/10.1002/2014wr016354

Wallace, C. D., & Soltanian, M. R. (2021a). Surface water-groundwater exchange dynamics in buried-valley aquifer systems. *Hydrological Processes*, *35*(3), e14066. https://doi.org/10.1002/hyp.14066

Wallace, C. D., & Soltanian, M. R. (2021b). Underlying riparian lithology controls redox dynamics during stage-driven mixing. *Journal of Hydrology*, *595*, 126035. https://doi.org/10.1016/j.jhydrol.2021.126035

Wallace, C. D., Tonina, D., McGarr, J. T., de Barros, F. P., & Soltanian, M. R. (2021). Spatiotemporal dynamics of nitrous oxide emission hotspots in heterogeneous riparian sediments. *Water Resources Research*, *57*(12), e2021WR030496. https://doi.org/10.1029/2021wr030496

Weiss, J. (1991). The dynamics of enstrophy transfer in two-dimensional hydrodynamics. *Physica D: Nonlinear Phenomena*, *48*(2–3), 273–294. https://doi.org/10.1016/0167-2789(91)90088-q

Yoon, S., Dentz, M., & Kang, P. K. (2021). Optimal fluid stretching for mixing-limited reactions in rough channel flows. *Journal of Fluid Mechanics*, *916*, A45. https://doi.org/10.1017/jfm.2021.208

Ziliotto, F., Basilio Hazas, M., Muhr, M., Ahmadi, N., Rolle, M., & Chiogna, G. (2025). Relevance of local dispersion on mixing enhancement in engineering injection and extraction systems in porous media: Insights from laboratory bench-scale experiments and modeling. *Transport in Porous Media*, *152*(3), 20. https://doi.org/10.1007/s11242-025-02155-7